Supplementary Figures

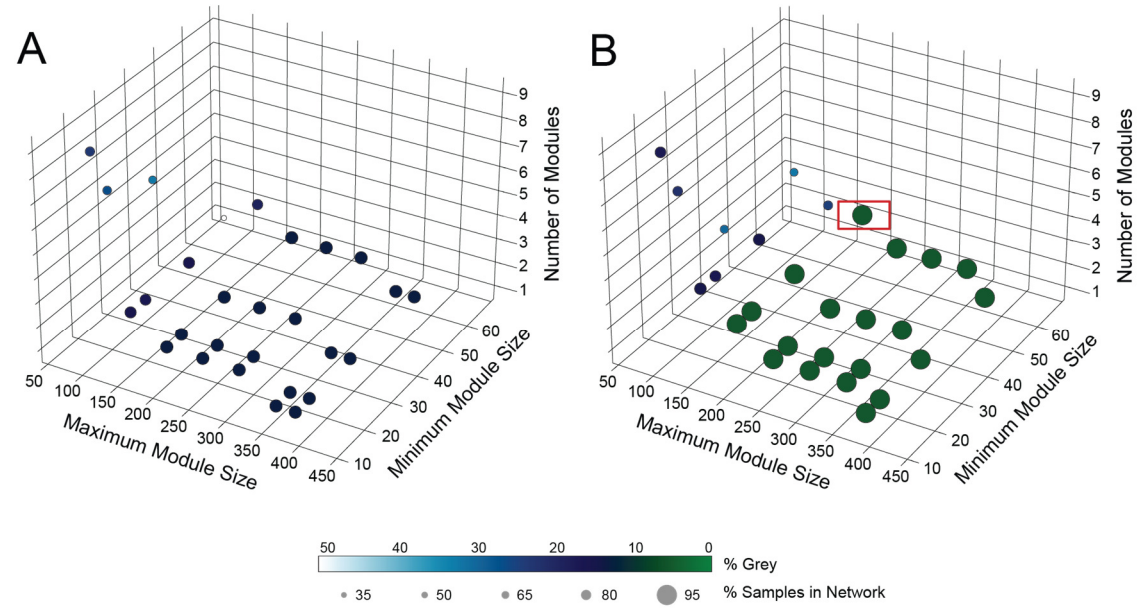

C

	Minimum Module Size	Maximum Module Size	Average Degree
13.26 %	5	200	25
13.26 %	10	200	25
13.26 %	25	200	25
13.26 %	50	200	25
13.26 %	5	250	25
13.26 %	10	250	25

Increasing % Grey

D

	Minimum Module Size	Maximum Module Size	Average Degree
5.31 %	**5**	**200**	**50**
5.31 %	10	200	50
5.31 %	25	200	50
5.31 %	50	200	50
5.31 %	5	250	50
5.31 %	10	250	50

Increasing % Grey

Figure S1. MONET M1 grid search and parameter selection. To select the hyperparameters used in MONET M1 clustering, a grid search of varying minimum module size, maximum module size, and average degree was performed. The percent of unassigned samples (% grey) produced in each combination are visualized as a 3D plot of minimum module size, maximum module size, and number of clusters at a desired degree of 25 (**A**) or 50 (**B**). The top performing parameter combinations as determined by minimal percent of unassigned samples (% grey) are provided in table format for a desired average degree of 25 (**C**) and 50 (**D**). Overall, assigning the desired average degree to 50 decreased the percent grey in each of the tested parameter combinations. The hyperparameters selected were minimal module size = 5, maximum module size = 200, and desired average degree = 50, as indicated by the red boxes in (**B**) and (**D**).

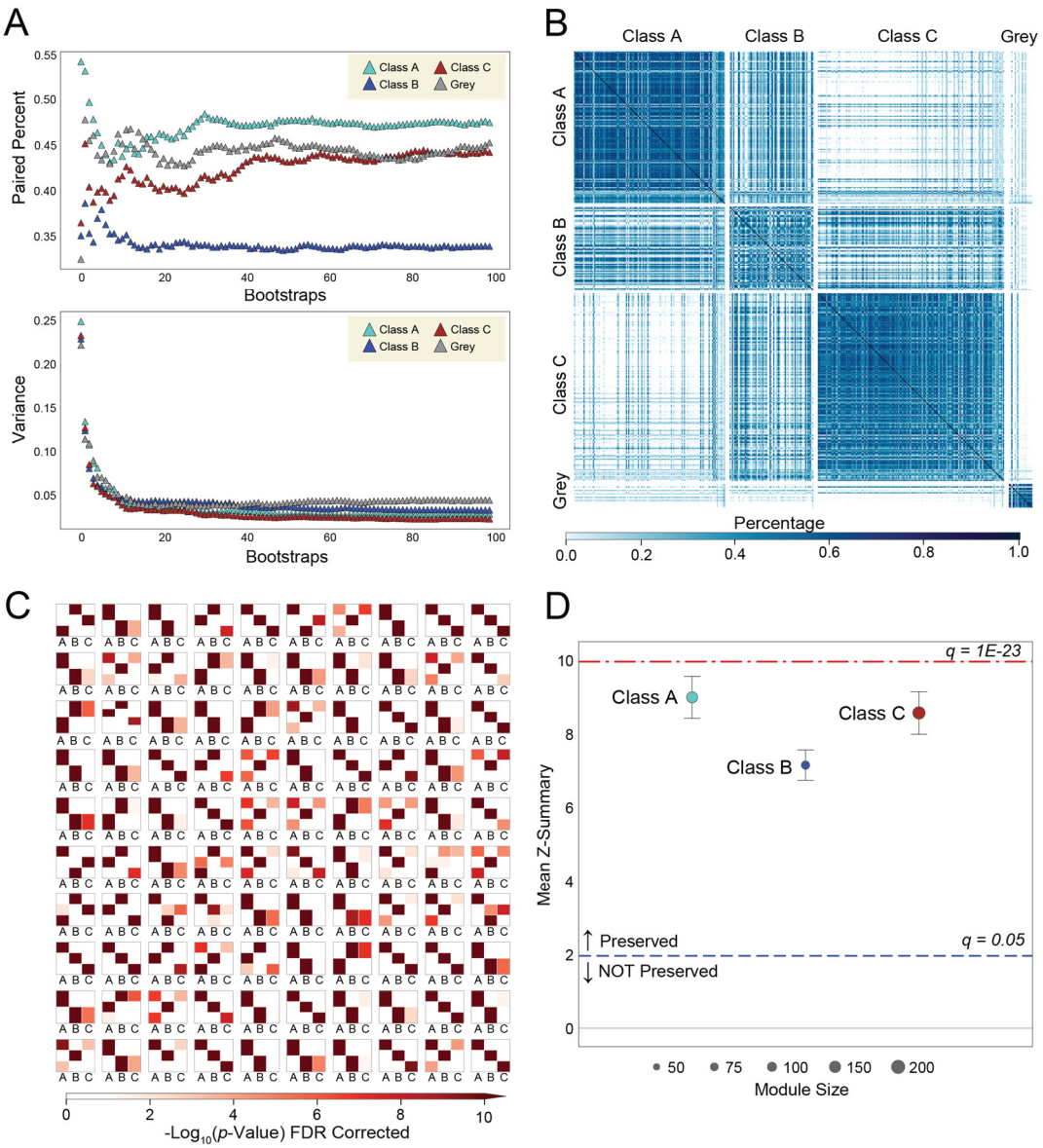

Figure S2. Validation of MONET M1 results using iterative bootstrapping. To validate the robustness of the MONET M1 clustering, we performed 100 rounds of bootstrapped reclustering. In each iteration, we withheld a random 20% of the samples and employed MONET M1 on the remaining 80% of MCI and AD cases. The paired percentage, i.e., rate at which sample pairs are assigned to the same cluster, termed the paired percentage, was calculated for every bootstrapped run (80-20 split). The average paired percentage per cluster and variance of the percentage were tracked to ensure the bootstrapping was well converged (**A**). A heatmap of the pairwise cluster rate showed three distinct clusters (**B**). Hypergeometric Fisher's exact test (FET) and module preservation were run on each of the MONET M1 reclustering steps with the original MONET M1 network as a reference. FET results revealed significant class-specific sample overlap (FDR-corrected $p<0.01$) across the 100 iterations (**C**). A mean Z-summary score was calculated and demonstrated that each of the MONET M1 classes were well preserved ($q < 0.05$) in each of the 100 bootstrap steps (**D**). Abbreviations: FDR, False Discovery Rate.

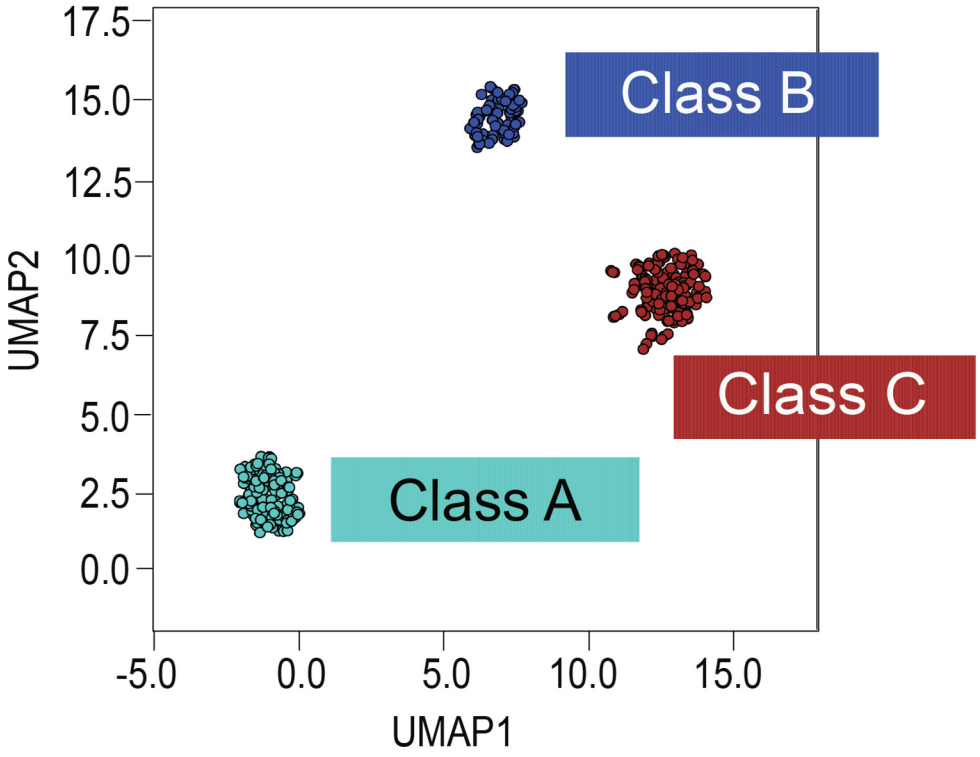

Figure S3. UMAP analysis reinforces proteomic classes of cognitive impairment. Uniform Manifold Approximation and Projection (UMAP) supervised clustering algorithm segregated cognitively impaired ROSMAP cases into three classes nearly identical to those formed by MONET M1. Only one of the 357 cases clustered differently between the algorithms, segregating into Class B with MONET M1 and Class C with UMAP.

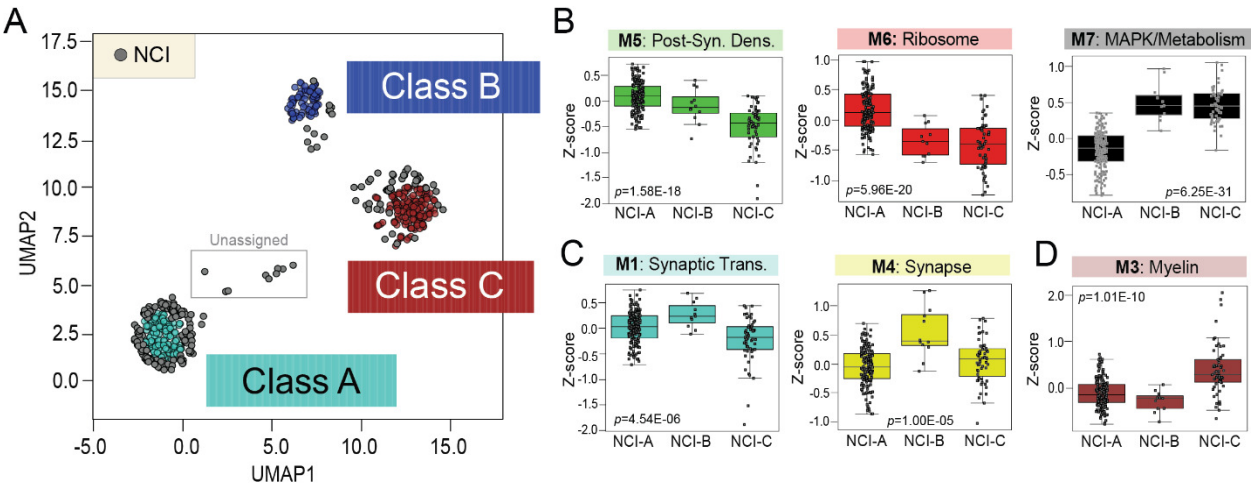

Figure S4. UMAP projections of cognitively intact cases highlight proteomic similarities between NCI and Class A. (**A**) Uniform Manifold Approximation and Projection (UMAP) of NCI samples onto the three classes of cognitive impairment based on proteomic profiles. Only one NCI sample from each of the five same-case pairs were included in this analysis, resulting in the projection of 215 NCI tissues. As expected, most NCI samples (n=149) clustered with Class A (NCI-A). Of the remaining NCI cases, 12 clustered with Class B (NCI-B), 45 with Class C (NCI-C), and 9 were unassigned. (**B-D**) Abundance levels (z-score) of select modules across the three NCI clusters. Module trends unique to Classes A, B, and C were reflected among these projected clusters, as shown in panels (**B**), (**C**), and (**D**) respectively. ANOVA p values are provided for each abundance plot. All modules depicted were significantly altered (p<0.001) across the four groups. Box plots represent the median and 25th and 75th percentiles, while data points up to 1.5 times the interquartile range from the box hinge define the extent of error bar whiskers. Abbreviations: NCI, No Cognitive Impairment; Post-Syn Dens, Post-Synaptic Density; Synaptic Trans, Synaptic Transmission.

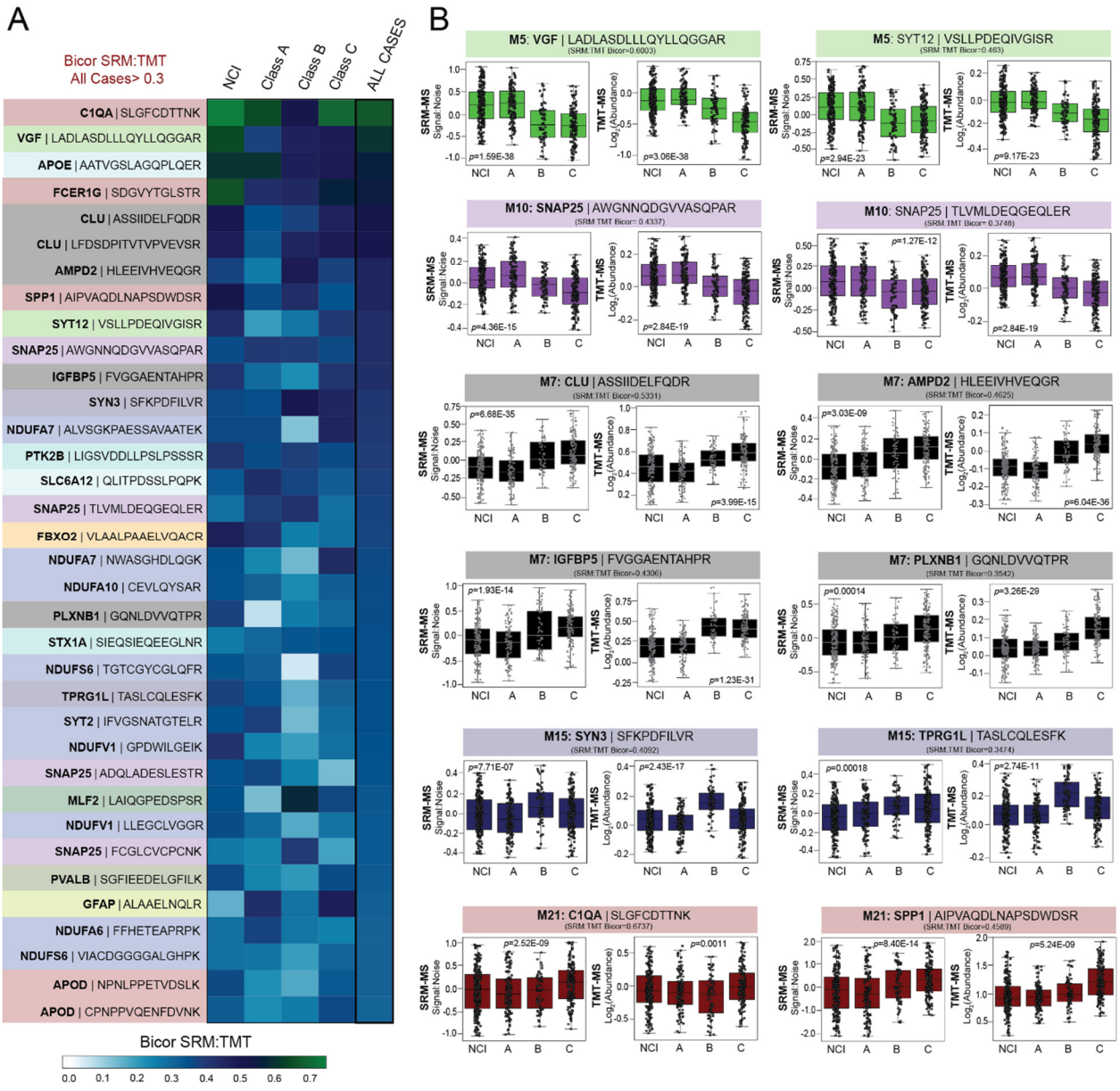

Figure S5. Targeted mass spectrometry reinforces class-specific protein signatures. We assessed the validity of our TMT-MS results using quantitative data from a previously published selected reaction monitoring (SRM) analysis of the same cognitively impaired ROSMAP cases. (**A**) Heat map depicting the correlation strength of SRM peptide levels with their corresponding TMT-measured protein abundances. Markers with highly concordant (*bicor* > 0.3) SRM and TMT levels across all cases are shown. (**B**) SRM abundance levels of select peptides aligned with the TMT-measured abundances of their corresponding proteins. The SRM data from these peptides consistently mirrored the TMT protein trends observed between classes. Box plots represent the median and 25th and 75th percentiles, while data points up to 1.5 times the interquartile range from the box hinge define the extent of error bar whiskers. Abbreviations: NCI, No Cognitive Impairment.

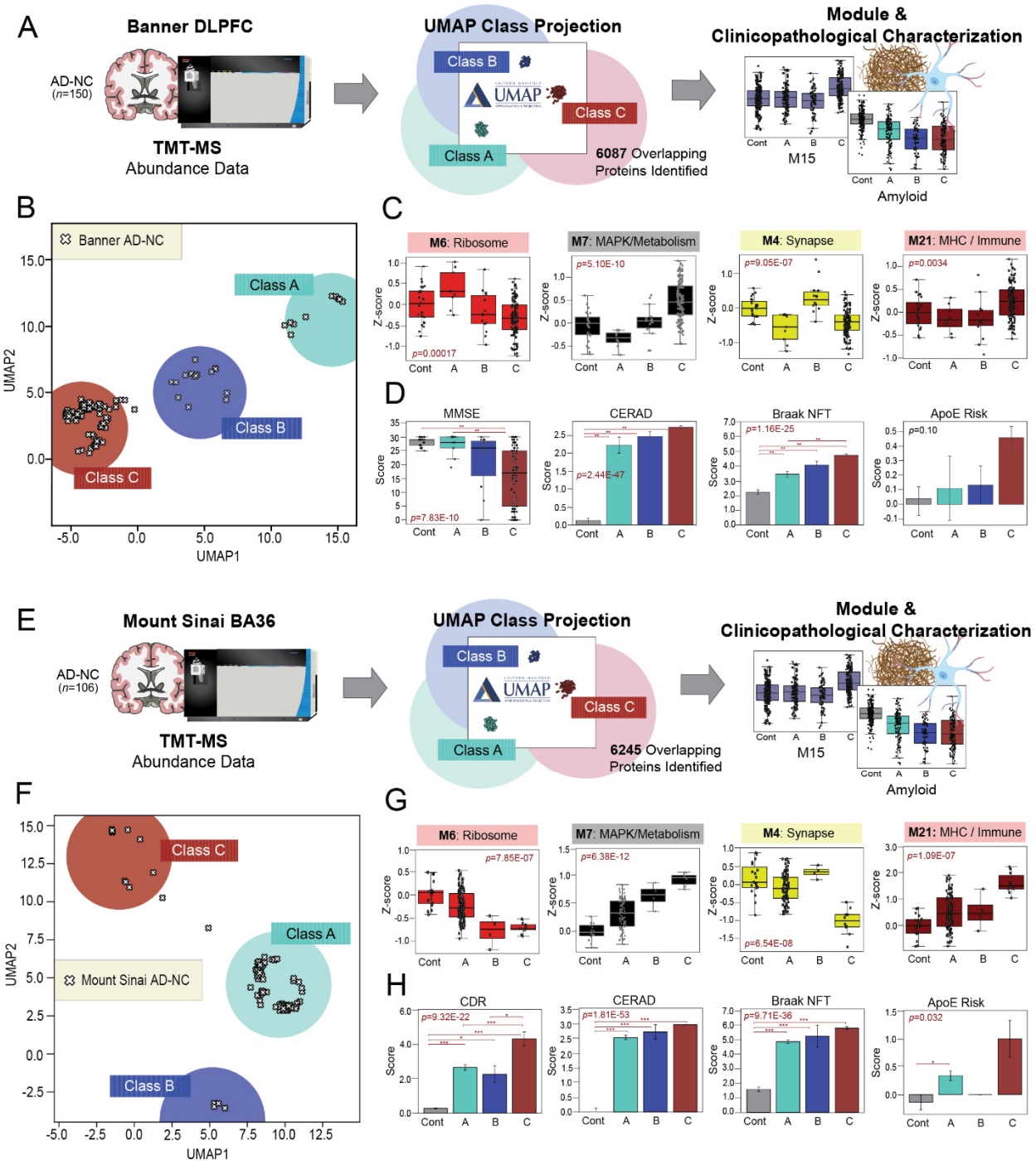

Figure S6. UMAP projections reinforce proteomic classes across additional cohorts and brain regions. We applied Uniform Manifold Approximation and Projection (UMAP) to brain tissues derived from additional independent brain banks onto the three classes of cognitive impairment based on proteomic profiles. TMT-MS abundance data (*n*=6,087 proteins) from Banner DLPFC tissues meeting pathological criteria for AD-NC (*n*=150 tissues) were used to perform the Banner class projections and subsequent module and clinicopathological class characterizations (**A**). UMAP ultimately classified 9 Banner cases to Class A, 15 to Class B, and 122 to Class C (**B**). Four cases were unassigned. Module abundance plots (z-score) across these projected Banner classes and 26 cognitively intact, pathologically clean control cases revealed expression trends similar to the original classes (**C**). ANOVA *p* values are provided for each module abundance plot. The Banner classes also featured clinicopathological

phenotypes consistent with those observed in the original ROSMAP classes (**D**). The ANOVA *p* value across groups is provided with asterisks indicating statistically significant Tukey post hoc pairwise comparisons (*, $p<0.05$; **, $p<0.01$; ***, $p<0.001$). The same projection method and class characterizations were completed using TMT-MS abundance data ($n=6,245$ proteins) from Mount Sinai BA36 tissues meeting pathological criteria for AD-NC ($n=106$) (**E-H**). In contrast to the Banner tissues, most of the Mount Sinai cases projected to Class A ($n=90$), while 4 were assigned to Class B, 10 to Class C, and 2 were unassigned. Yet, the three Sinai classes maintained very similar module abundance and clinicopathological characteristics to Banner and the original ROSMAP classes. All box plots represent the median and 25th and 75th percentiles, while data points up to 1.5 times the interquartile range from the box hinge define the extent of error bar whiskers. Abbreviations: Cont, Control; AD-NC, Alzheimer's Disease Neuropathological Change; TMT-MS, Tandem Mass Tag Mass Spectrometry; MHC, Major Histocompatibility Complex; MMSE, Mini-Mental State Examination; CERAD, Consortium to Establish a Registry for Alzheimer's Disease; NFT, Neurofibrillary Tangles; CDR, Clinical Dementia Rating Scale.